

## PREPARATION OF CeCo<sub>5</sub> ALLOY BY ELECTRO-DEOXIDATION IN A Co<sub>3</sub>O<sub>4</sub>-CeO<sub>2</sub> MOLTEN SALT

Q. ZHANG<sup>a, b\*</sup>, Y. LI<sup>a</sup>, R. SANG<sup>a</sup>, Z. CUI<sup>a</sup>, W. MO<sup>c</sup>

<sup>a</sup>Analysis and Testing Research Centre, North China University of Science and Technology, Tangshan 063210, China

<sup>b</sup>College of Metallurgy and Energy, North China University of Science and Technology, Tangshan 063210, China

<sup>c</sup>Yisheng college, North China University of Science and Technology, Tangshan 063210, China

The CeCo<sub>5</sub> alloy was successfully prepared using Co<sub>3</sub>O<sub>4</sub>-CeO<sub>2</sub> as raw materials. The composition of cathode product was analyzed by X-ray diffractometer. The morphology of cathode and its products were observed by field emission scanning electron microscope. The product prepared by electric deoxygenation of molten salt is mainly affected by the sintering temperature and electrolytic voltage. The CeCo<sub>5</sub> alloy can be prepared by the Co<sub>3</sub>O<sub>4</sub>-CeO<sub>2</sub> cathode body sintered at 850 °C and 1050 °C under 3.1 V electrolytic voltage, but the electrolysis process of the cathode sample sintered at low temperature is more complete, and the final product is also more pure. Pure CeCo<sub>5</sub> alloy can be obtained under 3.1 V electrolytic voltage for 20 h using Co<sub>3</sub>O<sub>4</sub>-CeO<sub>2</sub> as the cathode.

(Received November 1, 2018; Accepted April 11, 2019)

*Keywords:* Hydrogen storage alloy, Electro-deoxidation, CeCo<sub>5</sub>, Molten salt

### 1. Introduction

With the arrival of the fossil energy crisis, hydrogen energy has attracted more and more people's attention because of its pollution-free and abundant reserves, and hydrogen storage is a key step for the widespread application of hydrogen energy [1-3]. Justi and Ewe [4] found that LaNi<sub>5</sub> alloy can reversibly absorb hydrogen by electrochemical method for the first time, which began the study of hydrogen storage alloys and nickel-hydrogen(Ni-MH) batteries. In 1987, the composition of MnNi<sub>55</sub>-Co<sub>0.75</sub>-Mn<sub>0.4</sub>Al<sub>0.3</sub> was realized for commercial production. As a negative electrode material for batteries, hydrogen storage alloys must meet the following performance requirements: high capacity and discharge capacity, long cycle life, good stability in KOH electrolytes, good electrochemical catalytic activity and low price, etc [5-8]. Among the various AB<sub>5</sub> hydrogen storage materials, LaNi<sub>5</sub> is expensive, easy to corrode, and has poor cycle stability [9,10], CeNi<sub>5</sub> has the best stability but low capacity [11]. In comparison, the cyclic stability of metal Co replacing Ni has been greatly improved and the capacity is higher. Therefore, Co doped rare earth hydrogen storage alloys have attracted more and more scientists' attention [12].

Co's partial substitution for Ni can significantly improve the cyclic stability of the alloy, and the main reason is that Co's partial substitution for Ni can effectively reduce the lattice expansion after hydrogen absorption of the alloy, thus reducing the powder and corrosion tendency for the LaNi<sub>5-x</sub>Co<sub>x</sub> (X=0-3.5) alloy during the alloy's charging and discharging cycle [13]. Co also inhibits the dissolution of other elements such as Mn and Al into KOH solution. The higher the Co content, the less the amount of dissolution of Mn and Al in the lye, which increases the cyclic life of the alloy [14]. In addition, the study also found that Co is oxidized to Co(OH)<sub>2</sub> or HCoO<sub>2</sub><sup>-</sup> under strong alkali action during alloy discharge, however, during the charging process, it is reduced to metal Co, in the course of repeated charge and discharge, forming a thin layer of metal Co with good conductivity or its oxide film on the surface of the alloy, which improves the efficiency of charging and discharging and improves high rate discharge performance for the alloy [15]. Therefore, the feasibility study for the preparation of CeCo<sub>5</sub> by electric deoxygenation of molten

---

\* Corresponding authors: zhangqingjun@ncst.edu.cn

salt is carried out in this experiment. The effects of sintering temperature and electrolytic voltage on the preparation of  $\text{CeCo}_5$  by electric deoxygenation of molten salt are also studied.

## 2. Experimental

The corresponding mass of  $\text{Co}_3\text{O}_4$  and  $\text{CeO}_2$  are weighed at a ratio of Co to Ce atomic molar ratio of 5:1, acetone and 1 wt % PVB are added. Place them in a ball grinder, grind 6 h in the ball grinder, and then naturally dry in the air. Place the dried powder in an Agate mortar to grind and granulate, press the powder into  $\Phi 10$  body with 2.5 g under 30 MPa, and the round hole of  $\Phi 1$  is drilled in the center of the specimen. The molded specimens were sintered for 4 h at 850 °C, 1050 °C, and 1250 °C, respectively, cooled for use. Weigh 800 g anhydrous  $\text{CaCl}_2$  melt salt, fine mixing, sintered at 400 °C for 10 h, cooled for use.

## 3 Results and discussions

### 3.1. Effect of sintering temperature on the electrolytic products

Table 1 shows the porosity and bulk density of the specimen at different sintering temperatures. The results show that the porosity of the specimen decreases after sintering, and the body density increases. In addition, the results of Table 1 also show that the sample has similar porosity at sintering temperatures of 850 °C and 1050 °C, while the porosity decreases significantly and the bulk density increases significantly at sintering temperatures of 1250 °C. At different sintering temperatures, the microscopic morphology of the sample is shown in Figure 1. The figure shows that there is no significant difference between the microscopic morphology of the sample sintered at 850 °C and that of the unsintered sample, and the particle size is small. Compared with the sample sintered at 850 °C, the microscopic morphology of the sample sintered at 1050 °C showed significant changes, that is, the higher the sintering temperature, the larger the size of the sample particles.

Table 1. Porosity and density of pellets sintered at different temperature.

Sintering temperature (°C)	Porosity (%)	Bulk density ( $\text{g}/\text{cm}^3$ )
850	36.41	4.4654
1050	35.09	4.5023
1250	16.96	6.0122

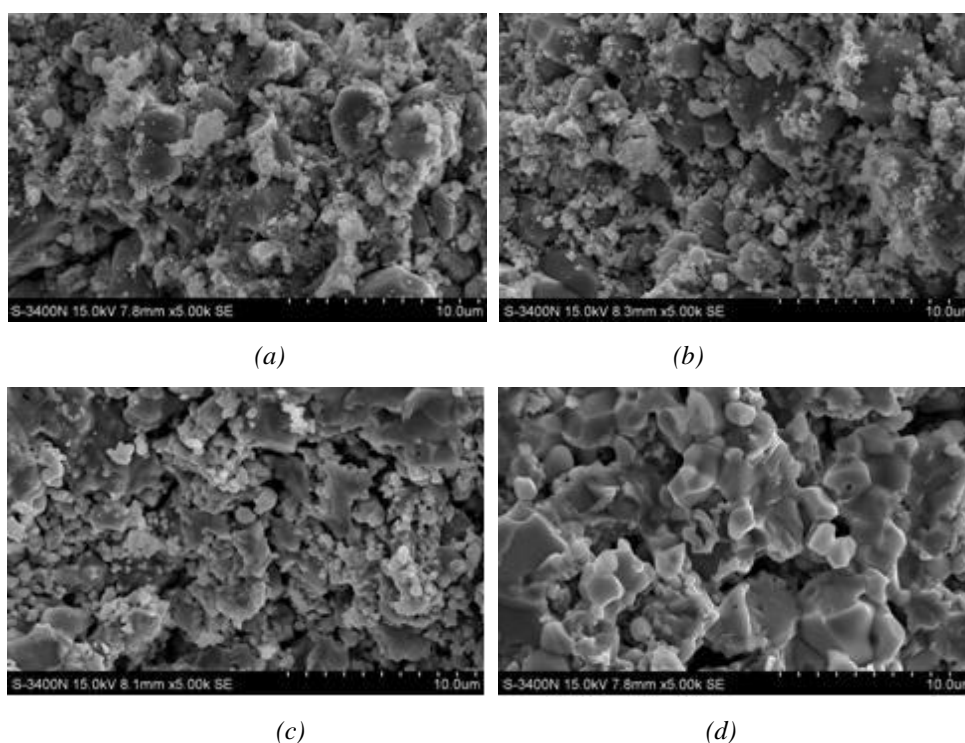


Fig. 1. SEM images of  $\text{Co}_3\text{O}_4\text{-CeO}_2$  pellets sintered for 4 h at different temperature. (a) unsintered; (b)  $850^\circ\text{C}$ ; (c)  $1050^\circ\text{C}$ ; (d)  $1250^\circ\text{C}$ .

The XRD results of the product after 3.1 V electrolysis at different sintering temperatures are shown in Fig. 2. It can be seen from the figure that the electrolysis products sintered at  $850^\circ\text{C}$  are mainly  $\text{CeCo}_5$  alloys, with only two  $\text{Ce}_7\text{Co}_{17}$  miscellaneous peaks, and the peak strength is very weak. The electrolysis products sintered at  $1050^\circ\text{C}$  are mainly  $\text{CeCo}_5$ , plus a small amount of  $\text{Ce}_7\text{Co}_{17}$ , and the alloying was relatively complete. In the XRD map of the electrolysis products sintered at  $1250^\circ\text{C}$ , no diffraction peaks of  $\text{CeCo}_5$  alloys were found, only a small amount of  $\text{Ce}_7\text{Co}_{17}$  alloys, and metal Co and  $\text{CeOCl}$ . The diffraction results show that the sample sintering at  $850^\circ\text{C}$  is beneficial to the formation of  $\text{CeCo}_5$  alloy.

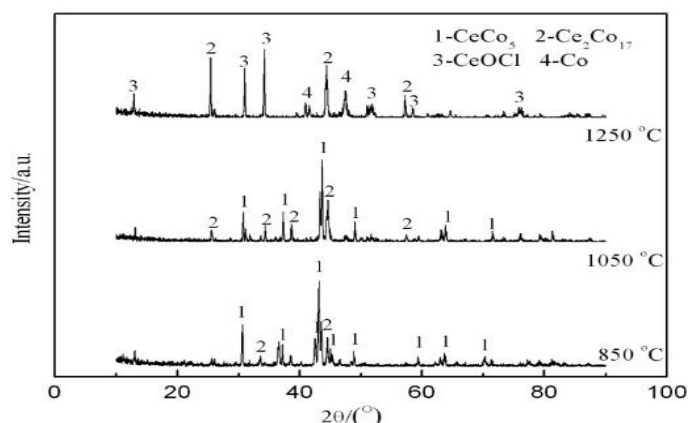


Fig. 2. XRD patterns of pellets sintered at different temperature and electrolyzed for 20 h.

At sintering temperatures of  $850^\circ\text{C}$ ,  $1050^\circ\text{C}$  and  $1250^\circ\text{C}$ , the micromorphology of the sample electrolysis product is shown in Figure 3. It can be seen from the figure that at the sintering temperature of  $850^\circ\text{C}$ , the electrolytic product particles of the sample are basically spherical, and a small number of grains form a more regular parallel hexahedral body type, the sample has large

pores, indicating that its alloying degree is higher. At a sintering temperature of 1050 °C, many burrs appear on the surface of the electrolytic product particles of the sample, which may be caused by impure alloys. At the temperature of sintering at 1250 °C, the particles of the sample electrolysis product were close to spherical, and the particles were relatively dispersed and small in size, indicating that the alloying degree was low, which is consistent with the results of the diffraction map.

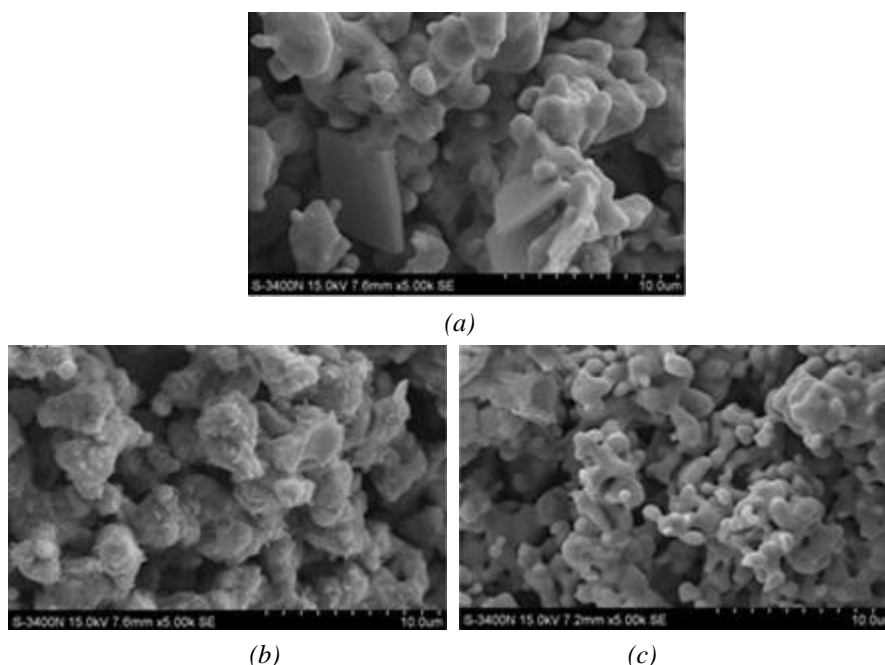


Fig. 3. SEM images of pellets sintered at different temperature and electrolyzed for 20 h (a)850 °C; (b)1050 °C; (c)1250 °C.

### 3.2. Effect of electrolytic voltage on the electrolytic products

Fig. 4 is the XRD patterns of the products at different electrolytic voltages. It can be seen from the figure that no  $\text{CeCo}_5$  alloy was found in the electrolytic product below 3.1 V, indicating that the  $\text{Co}_3\text{O}_4\text{-CeO}_2$  sintered sample can't be reduced to  $\text{CeCo}_5$  alloy. Under 2.1 V electrolytic voltage, the product contains diffraction peaks of  $\text{CeOCl}$ ,  $\text{CeO}_2$ , and metal Co, indicating that part of  $\text{CeO}_2$  is reduced to  $\text{CeOCl}$ , and  $\text{Co}_3\text{O}_4$  is completely reduced to metal Co. Under 2.8 V electrolytic voltage, no diffraction peak of  $\text{CeO}_2$  can be found, indicating that  $\text{CeO}_2$  has been completely reduced to  $\text{CeOCl}$ .

Under different electrolytic voltage, the morphology of the product is also quite different. At the sintering temperature of 850 °C, the cross-section morphology of the product after electrolysis for 20 h at different voltages is shown in Fig. 5. It can be found from the figure that after electrolysis for 20 h at the voltage of 2.1 V and 2.8 V, the morphology of the product is very irregular, the shape is different, and the size of the particles is also different, and the particle size of the product is relatively uniform at the voltage of 3.1 V electrolysis. Compared with the sample with lower electrolytic voltage, the size of grain increases, and the pores are large. From the previous analysis, it can be inferred that the sample alloying degree is relatively high.

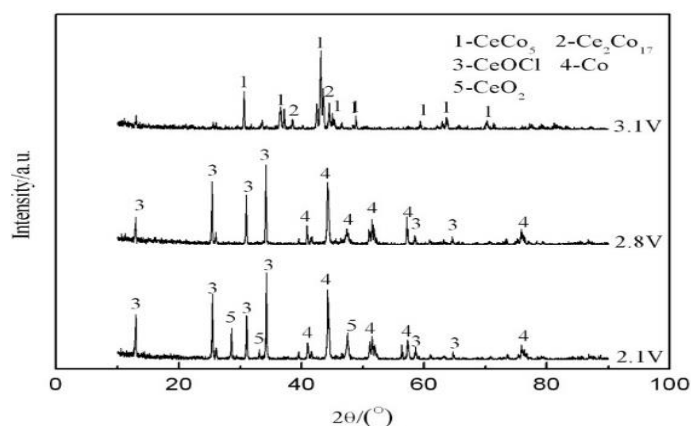


Fig. 4. XRD patterns of the pellets electrolyzed at different voltage.

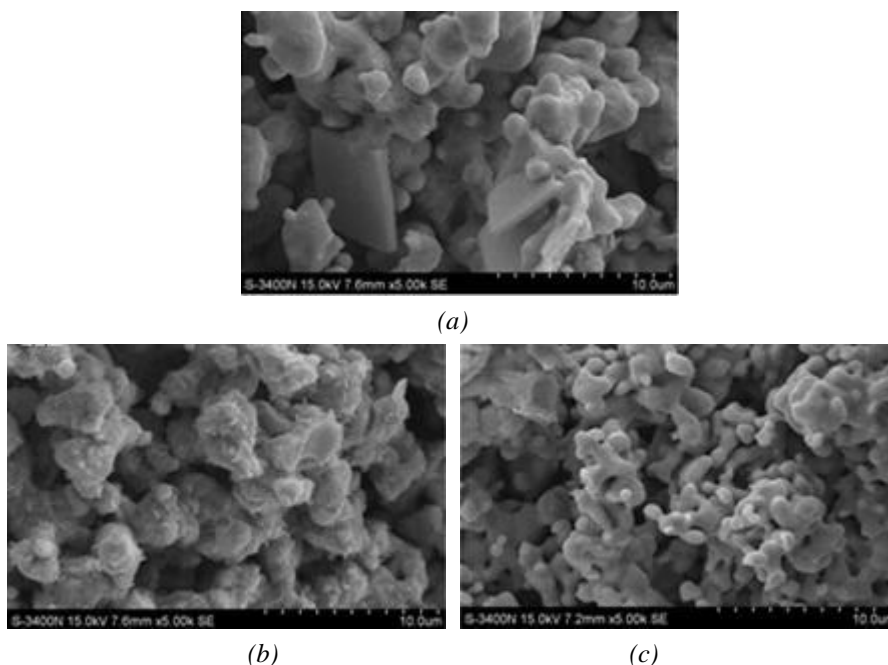


Fig. 5. SEM images of the pellets electrolyzed under different voltage.  
(a)2.1 V; (b)2.8 V; (c)3.1 V.

#### 4. Conclusions

The preparation of  $\text{CeCo}_5$  alloy by molten salt electric deoxidation was studied by using  $\text{Co}_3\text{O}_4\text{-CeO}_2$  as raw materials sintered at different temperatures. The results show that the  $\text{CeCo}_5$  alloy can be prepared by the  $\text{Co}_3\text{O}_4\text{-CeO}_2$  cathode body sintered at 850 °C and 1050 °C under 3.1 V electrolytic voltage, but the electrolysis process of the cathode sample sintered at low temperature is more complete, and the final product is also more pure. The specimen sintered at 1250 °C under the same electrolytic conditions, its product is mainly  $\text{Ce}_2\text{Co}_{17}$  alloy,  $\text{CeCo}_5$  alloy is not available. For the specimen sintered at 850 °C, the product becomes pure  $\text{CeCo}_5$  alloy under 3.1 V electrolytic voltage for 20 h. At less than 3.1 V electrolytic voltage,  $\text{Co}_3\text{O}_4\text{-CeO}_2$  can't be reduced to  $\text{CeCo}_5$  alloy.

### Acknowledgements

This work is partially supported by the National Natural Science Foundation of China (Grant No. 51874137) and the Natural Science Foundation of Hebei Province (Grant No. E2017209223).

### References

- [1] R. Hardian, C. Pistidda, A. -L. Chaudhary et al., *International Journal of Hydrogen Energy* **43**(34), 16738(2018).
- [2] D. G. Oliva, M. Fuentes, E. M. Borzone et al., *Energy Conversion and Management* **173**, 113 (2018)
- [3] P. Meena, M. Jangir, R. Singh et al., *Journal of Materials Research and Technology* **7**(2), 173 (2018).
- [4] H. Ewe, E. W. Justi, K. Stephan, *Energy conversion* **13**(3), 109 (1973).
- [5] T. Z. Si, Q. A. Zhang, *Journal of alloys and compounds* **414**(1-2), 317(2006).
- [6] E. Raekelboom, F. Cuevas, B. Knosp et al., *Journal of power sources* **170**(2), 520(2007).
- [7] M. S. Yahya, N. N. Sulaiman, N. S. Mustafa, *International Journal of Hydrogen Energy* **43**(31), 14532 (2018).
- [8] T. Y. Wei, K. L. Lim, Y. S. Tseng et al., *Renewable and Sustainable Energy Reviews* **79**, 1122 (2017).
- [9] G. Z. Kuang, Y. G. Li, F. Ren et al., *Journal of Alloys and Compounds* **605**(25), 51 (2014).
- [10] F. S. Yang, X. X. Cao, Z. X. Zhang et al., *Energy Procedia* **29**, 720 (2012).
- [11] R. Yamagishi, T. Kojima, S. Kameoka et al., *International Journal of Hydrogen Energy* **42**(34), 21832 (2017).
- [12] L. Dai, S. Wang, Y. H. Li et al., *Transactions of Nonferrous Metals Society of China* **22**(8), 2007 (2012).
- [13] Z. W. Liu, H. L. Zhang, L. L. Pei et al., *Transactions of Nonferrous Metals Society of China* **28**(2), 376 (2018).
- [14] M. Latroche, G. A. Percheron, Y. Chabre, *Journal of alloys and compounds* **637**(6), 293 (1999).
- [15] G. H. Rao, S. Wu, X. H. Yan et al., *Journal of Alloys and Compounds* **202**(1–2), 101 (1993).